



# Eco-friendly polyurethane foams based on castor polyol reinforced with açai residues for building insulation

Beatriz P. de Oliveira<sup>1</sup> · Lorena C. S. Balieiro<sup>1</sup> · Lana S. Maia<sup>2</sup> · Noelle C. Zanini<sup>3</sup> · Ericson J. O. Teixeira<sup>1</sup> · Monique O. T. da Conceição<sup>2</sup> · Simone F. Medeiros<sup>4</sup> · Daniella R. Mulinari<sup>1</sup>

Received: 20 July 2021 / Accepted: 13 December 2021 / Published online: 12 January 2022  
© Springer Japan KK, part of Springer Nature 2022

## Abstract

The search for environmental sustainability has stimulated the construction sector to look for natural materials with an ecological footprint, high strength/weight ratio, and better thermal and mechanical properties. Besides those properties, water absorption studies are necessary to reach these requirements. This research proposes to evaluate changes in the visual appearance, density, chemical structure, morphology, water absorption, porosity, and thermal and mechanical properties in castor oil-based polyurethane reinforced with açai waste (5–20 wt%). Results exposed that the addition of fiber to the PU reduced the pore size due to the increased cross-link density of PU foams caused by incorporating additional fiber groups, reacting with isocyanate groups. Also, the fibers were hydrogen bonded to the PU molecular chains via the interaction between the O–H of the fibers and the N–H of the PU foam. The water absorption of the biocomposites increased with time and with fiber loading; however, it did not surpass pure PU. The fiber addition improved crystallinity and hydrophobicity. The compressive strength presented a decreasing trend, while, for the impact test, an increase was observed proportionally to the açai residue content. Thus, the developed biocomposites can be a possibility for alternative eco-efficient building insulators.

**Keywords** Polyurethane foams · Açai residues · Water absorption · Thermal properties · Mechanical properties

## Introduction

The thermal and acoustic performance of buildings has been widely discussed in recent years, due to the importance of energy saving and noise control [1]. Furthermore, environmentally friendly materials are becoming increasingly significant in the building industry due to their enormous

environmental impact, responsible for 36% of final energy use and 39% of energy-related CO<sub>2</sub> emissions [2].

Thus, composite materials appear as an alternative to industrial waste and reduce environmental impacts [3]. Additionally, the advance in legislation related to the environmental aspect has caused industry changes to develop processes and products compatible with the environment, stimulating novel researches [2]. In this context, vegetable fibers such as agro-industrial residues become important alternatives for use as reinforcement material in polymeric materials [4, 5].

Among the agro-industrial residues, the açai seed is lignocellulosic biomass with no added value for the food industry, as only 10–20% of the pulp is used for the food industries. Açai is a palm found in northern Brazil, native to the Amazon region [6]. Açai or acai seed has been used for various applications such as charcoal production for methylene blue sorption, antioxidants for the treatment of carcinoma cells, biochar as a soil conditioner, enrichment of residual yeasts (*Saccharomyces cerevisiae*), and production of nanoporous carbon for CO<sub>2</sub> capture [7]. This reuse of solid agro-industrial waste has been defined as a biomass

✉ Daniella R. Mulinari  
daniella.mulinari@fat.uerj.br; dmulinari@hotmail.com

<sup>1</sup> Department of Chemistry and Environmental, State University of Rio de Janeiro (UERJ), Resende, RJ 27537-000, Brazil

<sup>2</sup> Department of Mechanic and Energy, State University of Rio de Janeiro (UERJ), Resende, RJ 27537-000, Brazil

<sup>3</sup> Center for Engineering, Modeling, and Applied Social Sciences (CECS), Federal University of ABC (UFABC), Santo André, Brazil

<sup>4</sup> Department of Chemical Engineering, Engineering School of Lorena, University of São Paulo, Lorena, SP 12602-810, Brazil

economy based on biomass conversion into high added value materials, such as chemicals and fuels [8]. However, it is necessary to investigate sustainable approaches and green technologies to dispose of these wastes and develop biotech-based products. Hence, an interesting route could be reusing this waste as a dispersed phase in polyurethane foams (PU) [4, 5, 9, 10].

Polyols and polyisocyanates are the main components of the vast family of polyurethane foams derivatives [11–13]. Cellular materials with a porous structure like polyurethane foams can have open or closed cells (pores), determining their applications. If the material has open cells and flexibility, the main destinations are furniture or bedding industries. If the material has closed cells and reduced thermal conductivity and density, the probable destinations are thermal insulation and building industries [14]. The type of reagents can influence the properties of polyurethane foams in their synthesis. Biopolyols derived from vegetable oils are more sustainable options than polyols derived from petroleum [15, 16]. An ecological mindset has been a trend in recent years in the choice of reagents for polyurethane synthesis. However, polyurethanes derived from biopolyols, such as castor oil, must have good properties that encourage their use over conventional options [17]. In addition, PU is a lightweight polymer that can be much more flexible and hydrophobic than other traditional lightweight materials, avoiding water absorption in construction materials [18, 19]. Table 1 evidenced the use of reinforcement different in polyurethane for use in buildings.

Castor oil-derived polyurethane stands out as a biodegradable polymer that replaces petroleum derivatives with vegetable oil as polymer monomers [11, 12, 14, 20]. By incorporating biomass into reactive castor oil-based polyurethane groups, the groups react with isocyanates, ensuring an optimal matrix–fiber interaction, improving their mechanical properties [20, 21]. Polyurethane composites based on castor oil reinforced with natural fibers have emerged in scientific research, mainly as adsorbent materials for oils, organic

solvents, and dyes [22]. Furthermore, this polymer can be applied to civil construction [23], lightweight thermal insulation [18], and sound-absorbing materials for door panels in automotive applications [24]. According to an analysis by Anh and Pasztory [25], thermal insulation materials are being more and more applied to the construction industry. The emerging use is due to these products aid in decreasing the use of heating or ventilation systems that consume much energy. In this context, polyurethane composites can be used for their low thermal conductivity and cost-effectiveness.

The objective of this article was to evaluate changes in the visual appearance, density, chemical structure, morphology, water absorption, porosity, thermal and mechanical properties in castor oil-based polyurethane reinforced with açai waste (5–20 wt%) biocomposites.

## Material and methods

### Materials

Fibers from açai seed residues were collected by Beraca Ingredientes Naturais S/A, located at Ananindeua, Pará-Brazil. Fibers were milled and sieved in 28 mesh apparatus. Both castor oil-based polyol (Biopol L40H, 531 mg KOH g<sup>-1</sup>) and isocyanate (Biopol p-MDI, 4,4-diphenylmethane diisocyanate, average functionality equal to 2.6, average molar mass equal to 349.9 g mol<sup>-1</sup>, solvent-free and average %NCO equal to 30–32) were provided by PolyUrethane (Minas Gerais, Brazil).

### Polyurethane foams and biocomposites processing

The PU biocomposites were obtained by methods proven in the literature [23, 26, 27]. Figure 1 shows a schematic representation of the adopted methodology. The polyurethane (PU) foam synthesis was made by manual mixing of castor oil-based polyol and prepolymer (1:1), in this order, for 50 s

**Table 1** Scientific studies involving different types of fibers as reinforcement in polyurethane for use in building

Polyurethane	Reinforcement	Application	References
Castor oil	Luffa fiber; glass wool; glass fiber	Sound insulation	[5]
Castor oil	Glass fiber	Beams	[1]
Castor oil	Bamboo fiber	Oriented strand board	[18]
Oil	Eucalyptus fibers	Insulation	[19]
Oil	Hemp fiber	Building insulation	[20]
Oil	Date palm	Building insulation	[21]
Oil	Alfa fiber	insulation	[22]
Polyurethane foam waste	Slag residues	The ecological mortar	[11]
Polyurethane foam waste	Pitch binders; cement or gypsum matrices	Prefabricated gypsum based	[13]

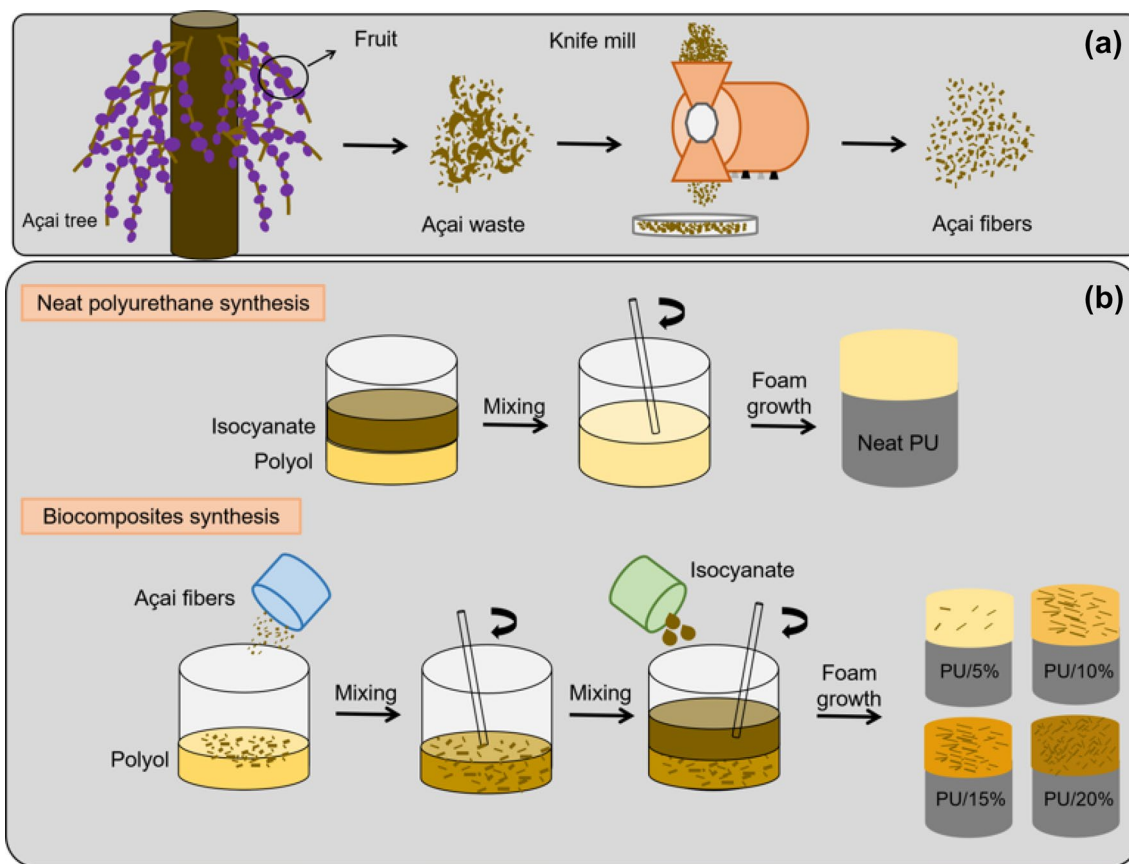


**Fig. 1** Schematic representation of the adopted methodology: **a** açai wastes' milling process, **b** synthesis process of PU foam and its biocomposites

at room temperature (27 °C) in plastic cups as molds. The polymerization occurred at 55 °C (exothermic reaction), and the polyurethane expansion occurred with pore formation (open and closed cells), forming a foam structure. The foams were removed from the plastic molds after one day (24 h) to guarantee their finished expansion structure [28]. Then, the foams were ready to be cut for the characterization tests. The PU biocomposites were obtained by the mixture of the açai fiber with the castor oil-based polyol, and subsequently, the prepolymer was added to the mixture. The subsequent steps for the biocomposite foams were analog to the pure PU foam described previously. The PU biocomposites were named PU/X%, where the X represents the percentage of açai fibers (5–20%) in the PU matrix.

## Characterization

### Optical microscopy, scanning electron microscopy and density

The ZEISS DISCOVERY V12 was the stereomicroscope (optical microscopy) used to explore the morphology of açai

and their dispersion in the foams and the surface pores of the PU foams. The SEM samples were gold-sputtered to prevent unwanted effects of electron beam loading during analysis [29]. HITACHI scanning electron microscope, with a tungsten filament, 5 kV, a low-vacuum technique and secondary electron detector was used. All samples were fixed on carbon tape. The density of pure PU foam and their biocomposites were determined in triplicate, and the samples were cut into cubic shapes (10 × 10 × 10 mm) and measured on a precision balance.

### Water absorption tests

The absorption capacity of water by PU and PU/X% foams was determined using a dynamic system in triplicate. The foam samples were dimensioned in 5 × 5 × 5 mm. Then, 0.30 g of material was immersed in 50 mL of water and submitted to manual agitation for 30–480 s, 24 h, and 48 h. After the contact time, the sorbent was removed and drained to eliminate excess water for 2 min. Lastly, the sample was weighed in a precision balance. Equations (1) and (2) were

used to obtain the absorption capacity ( $\text{g g}^{-1}$ ) and absorption efficiency (%) of the foams:

$$\text{Adsorption capacity } (\text{g g}^{-1}) = \frac{m_f - m_i}{m_i}, \quad (1)$$

$$\text{Adsorption efficiency } (\%) = \frac{m_f - m_i}{m_f} \times 100, \quad (2)$$

where  $m_f$  is the final sample mass and  $m_i$  is the initial sample mass.

#### Fourier transform infrared spectroscopy (FTIR)

A Thermo Scientific Nicolet IS5 spectrometer, Model ID3 Ge, with a transmittance mode, covering wavenumbers from 4000 to 600  $\text{cm}^{-1}$  and a spectral resolution of 2  $\text{cm}^{-1}$ , was used to perform the Fourier transform infrared spectroscopy (FTIR) analysis to investigate the functional groups and specific bands of the samples (açai, neat PU, and biocomposites). Attenuated total reflectance (ATR) spectroscopy was used. The deconvolution of two manually selected peaks (2850 and 2920  $\text{cm}^{-1}$ ) of the PU samples and biocomposites and their fits (Fit Peak 1 and Fit Peak 2, respectively) by Lorentzian deconvolution was done using OriginPro 9 software, obtaining a cumulative fit peak [30, 31].

#### Thermogravimetric analysis (TGA)

SDT Q600 thermogravimetric analyzer from TA Instruments was used to perform the thermogravimetric analysis (TGA) to investigate the samples' thermal properties (açai, neat PU, and biocomposites). The temperature range was 25–600 °C, under  $\text{N}_2$  atmosphere (10  $\text{mL min}^{-1}$ ) at a heating rate of 10 °C  $\text{min}^{-1}$ . The study of the heat-resistance index was made using Eq. (3) [32]

$$T_{\text{HRI}} = 0.49 \times [T_{5\%} + 0.6 \times (T_{30\%} - T_{5\%})], \quad (3)$$

where  $T_{\text{HRI}}$  is the heat resistance,  $T_{5\%}$  is the temperature at 5% weight loss, and  $T_{30\%}$  the temperature at 30% weight loss.

#### Differential scanning calorimetry (DSC)

The TA Instruments (USA) Q20 was used to perform differential scanning calorimetry (DSC) analyses. A temperature range of –80 to 300 °C under nitrogen at a 50  $\text{mL min}^{-1}$  flow rate and a heating rate of 10 °C  $\text{min}^{-1}$  in the ramp mode were used. Samples' weights of DSC runs were approximately 6 mg.

#### X-ray diffractometry (XRD)

The physical structures of the materials were evaluated by X-ray diffraction using a diffractometer (Rigaku, model Miniflex II). The measuring conditions were: CuK $\alpha$  radiation with graphite monochromator, 30 kV voltage, and 40 mA electric current. The patterns were obtained in 10–50° angular intervals with 0.05 steps and 1 s of counting time.

#### Mechanical tests

Impact tests were performed on an EMIC testing machine of the Charpy type with a 2.7 J pendulum. Five specimens were analyzed with dimensions according to the respective standard (ASTM D 6110-18). An EMIC testing machine (model DL2000) with pneumatic claws with a load cell of 5 kN was used to perform the compression tests, following the standard ASTM D 695-15, with 5  $\text{mm min}^{-1}$  to 20% deformation. The samples were cut into 50×50×25 mm size and placed between the two parallel plates for compression.

## Results and discussion

### Morphological analysis and density

The morphology and density of the foams were determined to investigate the surface of the açai fibers and determine their influence on PU matrix morphology. Figure 2 demonstrates the stereomicroscopy and SEM of the açai fiber. Figure 3 displays a graphical representation of the morphology of the PU foams and their biocomposites,

**Fig. 2** Stereomicroscopy and SEM of açai fibers

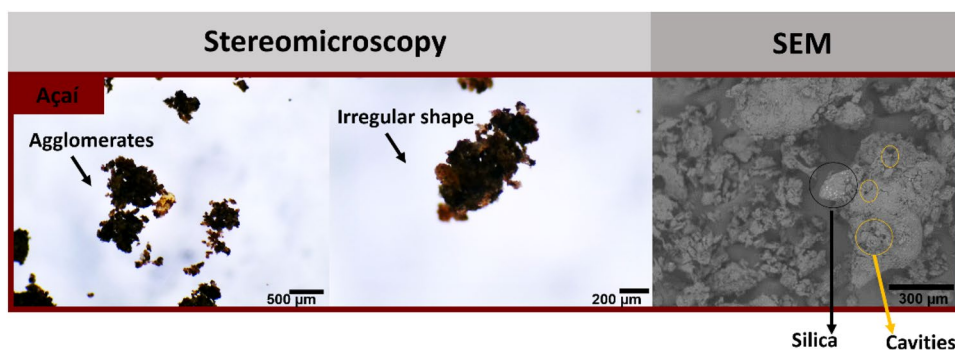
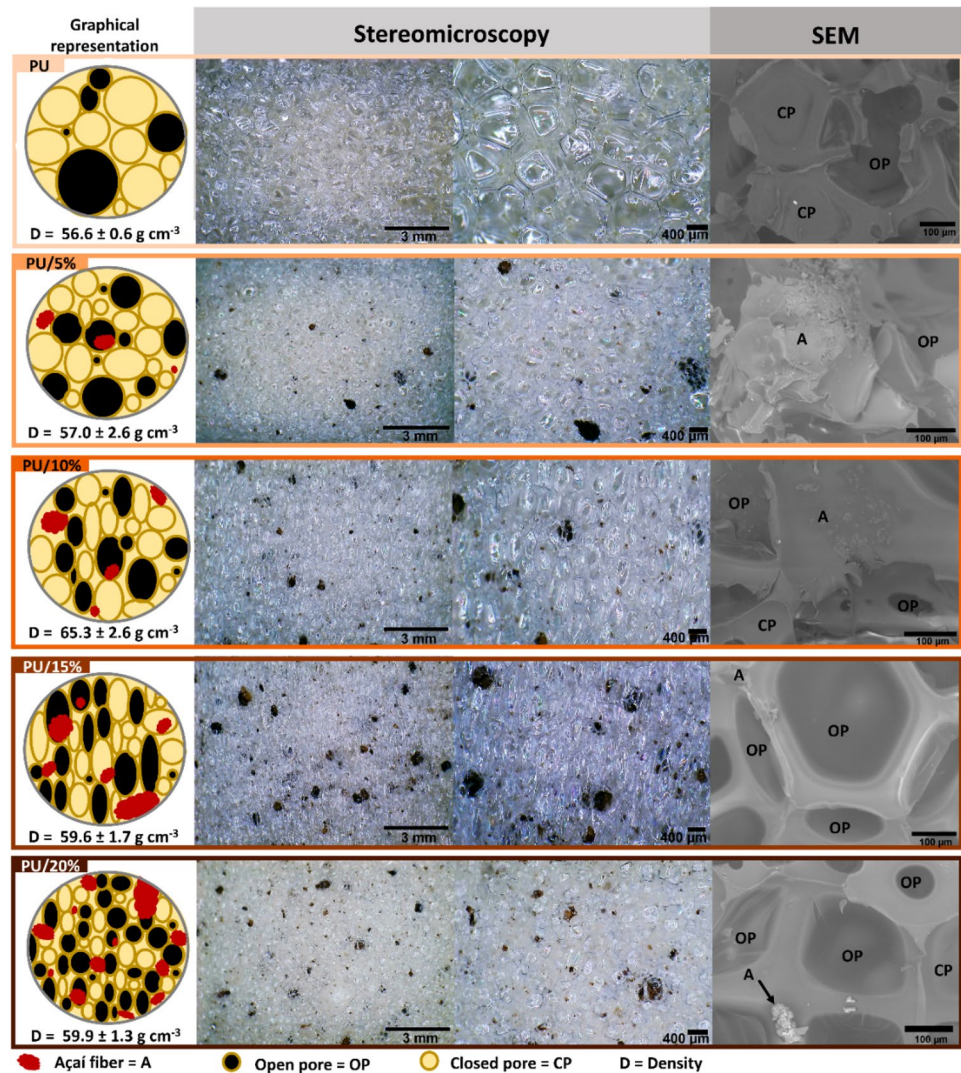


**Fig. 3** Graphical representation of morphology of PU foam and its biocomposites and their respective stereomicroscopy, SEM, and density



the density measurements, stereomicroscopy, and SEM images. Barbosa et al. investigated through the pycnometry technique the density of açai fibers for applications in the civil industry. They studied different grain sizes of açai fibers and obtained an average density value ( $1.49 \text{ g cm}^{-3}$ ). The fiber density can influence the mechanical, physical, and thermal properties due to their porous structure and contact area, affecting the fiber adhesion in composite structures [33].

An essential parameter for the fiber is the aspect ratio ( $L/D$ ) which consists of the relationship between the length ( $L$ ) and diameter ( $D$ ), and usually, this value is greater than 1 [34]. In the Supplementary Material section, Figure S1 evidences that açai fibers'  $L$  is greater than  $D$ ; therefore, a much higher  $L/D$  value is expected. When studying the aspect ratio of artemisia and macadamia fibers, Maia et al. [35] and Cortat et al. [31] observed smaller aspect ratios. In this study, the mean length ( $L$ ) and diameter ( $D$ ) values of

açai fiber were  $5661.4 \pm 1478.5 \text{ }\mu\text{m}$  and  $216.2 \pm 43.0 \text{ }\mu\text{m}$ , respectively. Thus, the aspect ratio of açai was equal to 26.2.

The stereomicroscopy images in Fig. 2 revealed that the açai fiber has a brown color, irregular shape, and clumps of fibers. SEM confirms such agglomeration and surface irregularity, presenting the porous nature of the fiber surface with cavities [36, 37]. The stereomicroscopy of the foams and its resulting graphical representation demonstrate that the dispersion of the açai fibers occurred in an inhomogeneous way (corroborating with the higher standard deviations of the densities of most of the biocomposite samples). That can be explained by the fiber hydrophilic nature and the hydrophobicity of the PU foam [33, 38]. Other authors have already seen the agglomeration of natural fibers as dispersed phases in a polyurethane matrix [22, 39, 40]. Moreover, factors such as the irregular surface geometry of the natural fiber and the difficulty in controlling the distribution of the fiber in the process of polyurethane expansion (from the mixture during

the synthesis reaction) may be determining factors for fiber agglomeration [22]. Soberi et al. [41] tested different mixing times to obtain a better dispersion of fibers in the PU matrix. Pearson and Naguib also used dispersant agents and synthesis methods of polyurethane in controlled environments in vacuum chambers [42].

According to studies, the insertion of natural fibers can reduce pore sizes and consequently induce the increased apparent density values of biocomposites concerning neat PU (Fig. 3) [35, 43, 44]. Oushabi et al. studied PU composites reinforced with palm fiber in contents of 5, 10, and 20% (w/w) for thermal coating in building applications. The authors observed that the increase in foam density with fiber loading was related to a slight increase in thermal conductivity, small enough that its application would still be considered over conventional thermal insulators [45].

Additionally, parameters such as cell diameter and cell wall thickness of samples can be analyzed as described in Table S1 and Figure S1. The results revealed that the greater the amount of fiber in the PU matrix, more significant was the reduction in these values that could be noticed. However, this behavior did not occur gradually, since the dispersion of the fibers occurs heterogeneously. When evaluating the PU foams reinforced with açai fiber developed by Martins et al. [7] (which has the same granulometry as the proposed samples in the present paper), a reduction in these values can be observed as a more significant amount of filler is added. The authors observed that, regarding cell diameter, neat PU and PU with 20% of fiber obtained  $152 \pm 61 \mu\text{m}$  and  $119 \pm 54 \mu\text{m}$ , respectively, while the cell wall thickness for the same foams was  $100 \pm 72 \mu\text{m}$  and  $42 \pm 13 \mu\text{m}$ . This behavior is due to increase in viscosity during the polymerization process that induces the formation of more centers of nucleation. The nucleation effect promotes an irregular morphology in a way that composites presented with thinner cell walls and a decrease in cell wall thickness. A similar behavior can be seen in other papers [46, 47].

The PU/20% sample presented the smallest pores and the lowest standard deviation concerning density, displaying better reinforcement dispersion for higher fiber contents. Better dispersion of fibers might signify interaction in terms of matrix/fiber interface due to the free hydroxyl groups present in the cellulose of the açai, interacting with the isocyanate of the PU [35]. Given this explanation, the interfacial

interaction between fiber/PU matrix can be through chemical reactions [48, 49]. Moreover, compared to the pristine PU, the biocomposite foams exhibited decreased pore diameter, improved pore frequency, and a tendency of density enhancement with the açai fiber loading. This may be a consequence of the dispersed phase of açai in the PU matrix when the expansion process happens during the foams' synthesis, causing a more prominent packing of its structures, reducing the volume of the pores (and consequently their diameter). Zanini et al. [44] mentioned that the viscosity of the polyol and isocyanate mixture in the expansion reaction process of PU foams increases with the insertion of a disperse phase. With this, the density of the foam obtains higher values. Besides, the density/pore size correlation was seen in Costa et al.'s [50] study with PU matrix and pineapple crown fibers reinforcement, which mentioned the indirectly proportional relationship between pore size and density with the insertion of natural fibers. The image obtained by SEM of the pure PU demonstrated the presence of open and closed pores (also seen by stereomicroscopy). In the SEM of the biocomposite samples, the presence of open pores was more evident near the açai fibers in different ways: incorporated into the matrix (for PU/5%, 10%, and 15%) and the fiber evident on the surface (for PU/20%).

### Water absorption tests

Polyurethane must have a low water absorption capacity, as water molecules change the structure and properties of both the matrix and the fibers, interfering with their interaction, quality, and durability [51]. Water absorption by porous materials depends on the structure and hydrophobicity of the material [52]. With the addition of fibers, polar groups are added to the material structure so that the hydrophobic character of the foam is affected [50, 53]. The contact angle of a water droplet in the foams' surface can indicate if the material is hydrophilic, hydrophobic, or superhydrophobic (Fig. 4). Table 2 shows the contact angle (CA) of the materials.

As seen in Table 2 and according to Fig. 4, all samples presented a  $\text{CA} > 90^\circ$ , which means they were all hydrophobic. It is worth mentioning that the insertion of 20% of açai fiber decreased the CA value due to the lignocellulosic fibers' hydrophilic nature (which character does not interfere

**Fig. 4** Schematic of hydrophilic, hydrophobic, and superhydrophobic surfaces

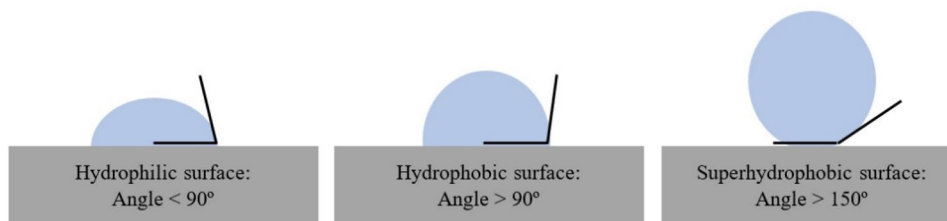


**Table 2** The measurements of contact angle between water and the surface of materials

Samples	Contact angle (°)
PU	102.33 ± 9.45
PU/5% açai	103.01 ± 17.55
PU/10% açai	110.70 ± 7.47
PU/15% açai	114.51 ± 0.72
PU/20% açai	98.34 ± 21.18

with the increased CA values until the addition of 15% reinforcement). Also, the high fiber content can increase the roughness of the biocomposite and favor the entry of water molecules during the measurement process [43]. Thus, it was possible to observe that most biocomposites are more hydrophobic than pure PU. Silva et al. [23] and Martins et al. [22] also evidenced a similar behavior when rubber powder waste and palm residues were added to the PU, respectively. However, Calegari et al. [54] and Costa et al. [50] observed a decrease in the contact angle when adding fibers from agro-industrial residues and wastepaper to the PU.

Figure 5a, b shows pure PU and PU7X% water absorption capacity ( $\text{g g}^{-1}$ ) and efficiency (%). Analyzing the data, biocomposites had lower performance when compared to pure PU, but the PU/5% was the composite with lower capacity and efficiency. The low absorption of water in the composites than pure PU might be due to the higher frequency of pores per area, disfavoring the water/matrix interaction [7], which can favor its application in civil construction. The lower water absorption of biocomposites can be associated with adhesion of the fiber/matrix interfaces, a greater affinity between water/polymer than water/fiber, and fewer voids due to the presence of fiber [55]. By increasing the amount of reinforcement in the PU, the water absorption efficiency increased. Nonetheless, it did not surpass pure PU.

An opposite behavior was observed by Calegari et al. [54] and Atiqah et al. [56], where the addition of fibers to the PU increased water absorption when compared to the pure PU.

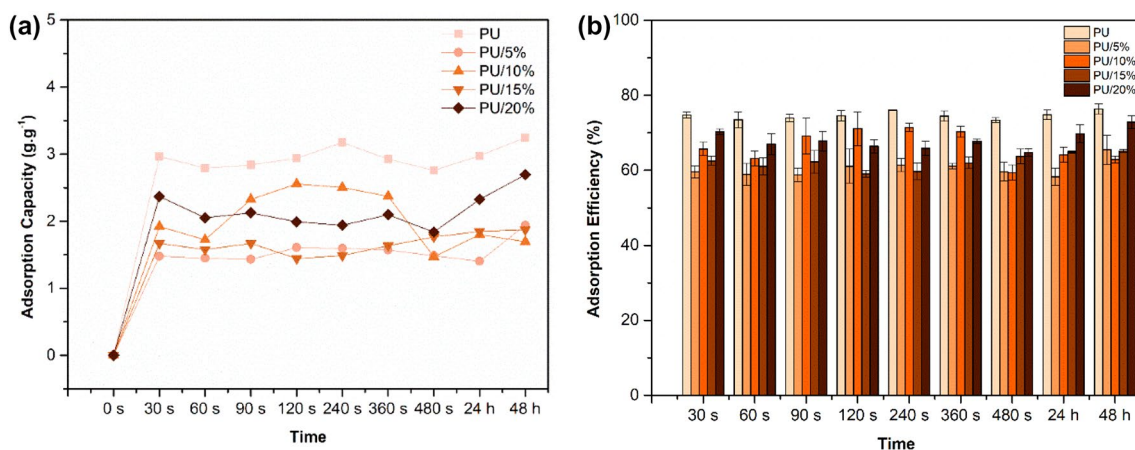
Another explanation can also be that the water absorption of the biocomposites is lower than that of pure PU. The açai fibers used in this work are *in natura*, i.e., they did not undergo any surface modification or treatment. Generally, alkaline treatments or bleaching can favor delignification and the removal of the superficial waxy layer of the fiber [57–59]. Although the fiber is a hydrophilic material, the *in natura* composition of the açai containing higher levels of lignin (usually insoluble in water [60]) and wax may also have interfered with water absorption. According to Barbosa et al. [33], the moisture content of açai fibers between 8 and 200 mesh is 3.75%, and values below 5% moisture content are recommended for fibers as dispersed phases in composites. Low moisture content values can decrease heat transport to the central region of the composite [33], which can be considered for applications as building insulators.

### Fourier transformed infrared spectroscopy (FTIR)

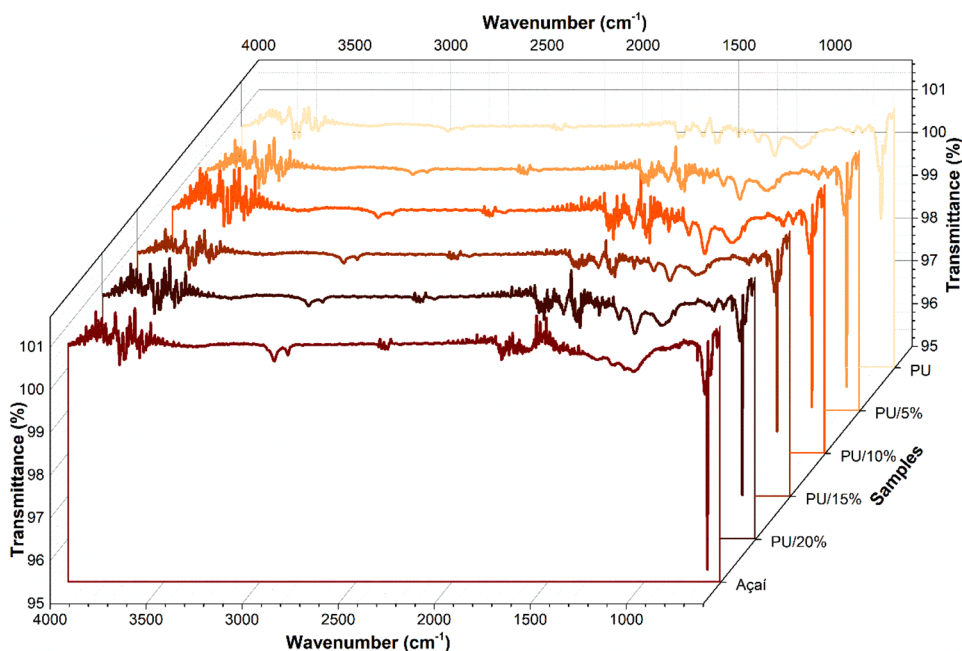
FTIR is an interesting technique to evaluate the surface functionality of pristine PU and biocomposites with different açai loadings utilizing specific wavenumbers [61]. Figure 6 exemplifies the FTIR of the samples.

Figure 6 evidences the expected bands for the spectrum of the pristine PU sample. The polyurethanes have urethane groups in their molecular chain, obtained through the reaction of its components during expansion, between the isocyanate group and the hydroxyl present in the polyol [62]. Similar bands for PU foams were found in the literature and can be seen in Table 3.

However, some changes in the characteristic PU bands were found in the biocomposite foams with the insertion of açai. The spectra of açai fiber *in natura*, i.e., without

**Fig. 5** Water absorption capacity (a) and absorption efficiency (b) of PU and biocomposites as a function of time

**Fig. 6** FTIR Spectra of the pristine PU and the biocomposite samples



**Table 3** Bands of the FTIR spectra of PU and their characteristics

Band (cm <sup>-1</sup> )	Attribution	Component	References
3900–3700	Noisy bands of –OH stretching	–	[46]
2850 and 2924	C–H stretch	–	[47]
1714	C=O stretching vibration	Urethane bridge	[48]
1600	C–N vibration	Urethane linkages	[49]
1592	C–C vibrations in aromatic rings	Isocyanate	[27]
1530	Stretching and bending vibration of N–H	Urethane linkages	[49]
1413	C–C stretch of aromatics	Urethane group (–NHCOO–)	[50]
1020–1070	Carbon–oxygen bond	Castor oil polyester polyol	[27]
1068	N–CO–O stretching	Urethane group (–NHCOO–)	[50]
817	C–H bond of aromatic rings	Isocyanate	[27]
754	C–H bond of aromatic rings	Isocyanate	[27]

any chemical treatment, presented similar bands to studies in the literature [7, 37, 63]. According to Tavares et al. [37], the chemical composition of açai is mostly cellulose (41.3%) and lignin (40.2%), and to a lesser extent hemicellulose (11.5%), moisture (8.8%), and ash (1.9%). Table 4 reunites the bands of açai fiber found in this work according to its chemical composition, compared to natural fibers (açai included) in the literature.

In their article, Martins et al. [7] mentioned that the açai fiber, as a dispersed phase, can cause changes through covalent or hydrogen bonds (H bonds) in the matrix. Such modifications might be due to the organic chemical composition of the açai fiber, with an endocarp rich in lignin and hemicellulose [36] endorsing the bands found in Table 4. The perturbation in the lengths of the 3700–3300 cm<sup>-1</sup> range in the biocomposites may be indicative of a reaction between the –OH groups of the açai with the isocyanate of the

polyurethane matrix, with a bond occurring between the cellulose of the natural fiber and the –NH group of the urethane [35]. As other evidence of the fiber amidst the matrix, the 680 cm<sup>-1</sup> band characteristic of the fiber remained intense in the biocomposites and a gradual effect of increasing peak intensity with fiber loading in the 2920 cm<sup>-1</sup> and 2340 cm<sup>-1</sup> bands, with highlights for the PU/15% and PU/20% samples most similar to açai in this wavenumber range. Figure 7 demonstrates the effect of the dispersed phase in the polyurethane matrix in the region between the peaks at 2850 and 2920 cm<sup>-1</sup> corresponding to Fit Peak 1 and Fit Peak 2, respectively.

Although there was no appearance of bands in the region of deconvolution analysis, the Fit Peaks 1 and 2 showed a gradual increase in the intensity of absorbance with the insertion of açai, evidencing the influence of reinforcement in the PU matrix, especially concerning Fit Peak 2



**Table 4** Bands of the FTIR spectra of açai fibers and their characteristics

Band (cm <sup>-1</sup> )	Attribution	Component	Fiber	References
3500–3200	Characteristic perturbations of residual moisture and stretching of –OH groups referring to hydrogen bonds	Cellulose, hemicellulose, lignin, and extractives	Açaí	[7, 34, 35]
2920	C–H starch	Cellulose	Açaí	[52]
2340	Stretching of –CH both symmetrical and asymmetrical in saturated hydrocarbons	Hemicellulose and cellulose	Açaí	[51]
1722	C=O stretching of carboxyl	Lignin and hemicellulose	Açaí	[35]
1640	Aromatic ring	Lignin	Açaí	[7]
1580	Tension of the C=O of the carboxylic acid and ester	Hemicellulose	Açaí	[51]
1453	CH deformation	Lignin	Açaí	[7, 35]
1272	C–O guaiacyl ring	Lignin	Açaí	[35]
1112–1030	C–H for in-plane deformation of the syringyl unit	Lignin	Açaí	[35]
680	C–OH out-of-plane bending	–	Hemp fibers	[53]

(2920 cm<sup>-1</sup>) which can be attributed to cellulose (Table 3). Cortat et al. [31] also found an increase of a fitted peak by this method with macadamia fibers in a polypropylene matrix.

### X-ray diffractometry

Figure 8 displays the physical characteristics of pure PU and its biocomposites obtained by the X-ray diffraction technique. The X-ray diffractograms of pure PU and biocomposites showed an extended peak in the region  $2\theta = 19^\circ$  and the absence of narrow peaks, revealing the amorphous character of the polyurethane foam. The addition of fibers to PU caused a broad peak compared to pure PU, associated with the açai residues due to cellulosic material with semicrystalline regions [64]. Thus, the displacement related to  $19^\circ$  is attributed to the chemical interaction between the pure PU and the fiber content. However, the fiber's content influenced the intensity of these peaks due to the lack of homogeneity during fiber dispersion [50]. Gandara et al. [20] observed a similar behavior when sugarcane bagasse fibers were added to the PU.

### Thermogravimetric analysis (TGA)

The thermogravimetric analysis (TGA) gives thermogravimetric curves (TGA) (Fig. 9a) and their derivatives (DTG) (Fig. 9b) of the açai seed fiber, neat PU, and biocomposites. Table 5 demonstrates the values of the percentages of weight loss in the respective temperature range of materials.

The TGA curve for açai seed fibers (Fig. 9a) indicated that the first thermal event occurred around 100 °C due to the OH group of the fiber, confirming the 3500–3200 cm<sup>-1</sup> band found in the FTIR analysis [65]. The second thermal event occurred between 200 and 300 °C, attributed to hemicellulose degradation and low molecular weight lignin. The

third thermal event occurred above 300–340 °C due to the decomposition of cellulose, which requires a high-temperature range because the decomposition of lignin occurs slowly [20].

The TGA curve for neat PU and biocomposites presented a similar trend and thermal stability up to 200 °C. The first thermal event occurred between 200 and 300 °C and is associated with the decomposition of urethane groups [22, 23]. The second thermal event occurred around 350 °C, and it is more evident for the biocomposites with more significant fiber content; these small peaks are associated with the decomposition of hemicellulose, lignin, and cellulose derived from the açai seed fiber. The maximum decomposition rate of these steps occurred at 325 and 356 °C, similar to the results found in the article of Członka et al. on polyurethane foams for insulating applications reinforced with eucalyptus fibers [66]. The third thermal event is assigned to the decomposition of C–C bonds, remaining materials from the first degradation step, and ester bonds present in the polyol. The degradation step occurs with the maximum at 455 °C for PU and 470 °C for the biocomposites [27]. Moreover, Table 5 demonstrates that the fiber insertion offered the PU matrix improved degradability for each temperature interval, as seen by Gu, Sain, and Konar in their study about biopolyol-based polyurethane with hardwood pulp for insulation applications [67].

Another interesting way to assess the thermal stability of biocomposites is to calculate the heat resistance index. The heat resistance index is the physical heat tolerance temperature of a polymer, which was determined using the method proposed by Icduygu et al. [32]. Table 6 provides the values for the heat resistance index ( $T_{HRI}$ ) of pure PU and biocomposites, calculated from thermograph data for the 5% ( $T_5$ ) and 30% ( $T_{30}$ ) weight losses of Fig. 9.

A slight increase in the biocomposites' thermal resistance was noted compared to pure PU due to insertion fibers

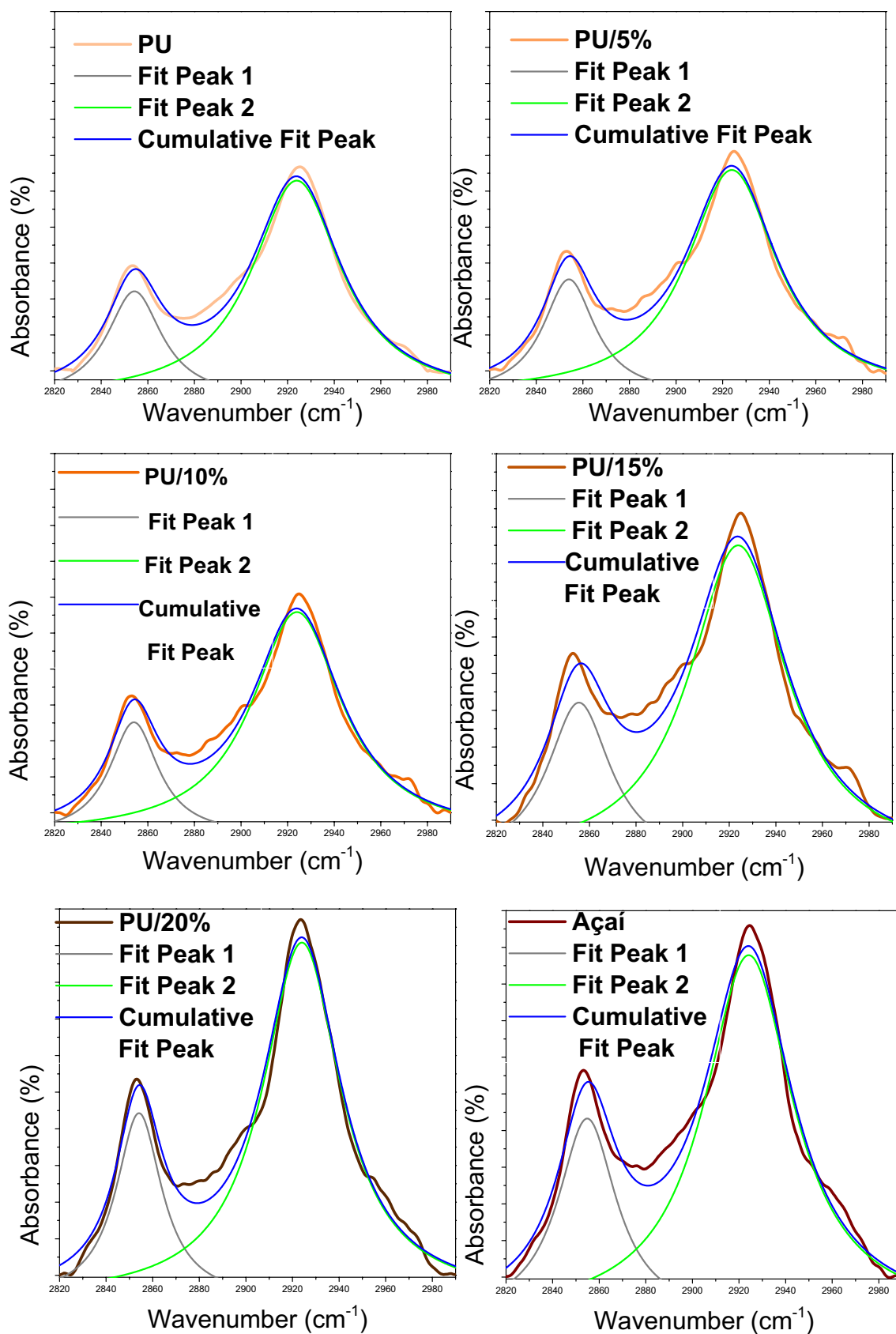
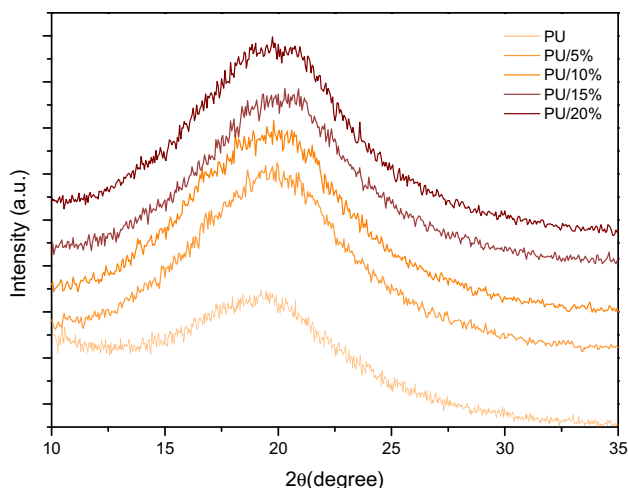


Fig. 7 Deconvolution of 2920 cm<sup>-1</sup> and 2340 cm<sup>-1</sup> bands of PU and its biocomposites



**Fig. 8** XRD of neat PU and biocomposites samples

in the matrix, except for PU/15%. This fact demonstrates that fibers' addition in the polyurethane matrix promotes better thermal stability at temperatures reaching 30% of weight loss for biocomposites. These results demonstrate that the biocomposites present better thermal properties for building insulation than the pristine PU foam.

### Differential scanning calorimetry (DSC)

DSC analyses were carried out to justify the effect of açai waste on castor oil-based polyurethane. DSC curves for neat PU, pure açai fibers, and biocomposites with açai concentration varying from 5 to 20 wt% are shown in Fig. 10. All curves showed a beta transition from  $-80$  to  $-75$  °C. The beta transition intensity varied with the introduction of açai fiber in the biocomposites, related to the  $H_2O$  molecules present in açai fibers, capable of reacting with the  $-NCO$  groups. This reaction improves the movement of molecules, influencing the beta transition and the  $T_g$ , as shown in Fig. 8. The thermogram of the neat açai fiber shows a second-order transition at  $0$  °C, attributed to humidity retained in the fibers. The well-defined characteristic peak shows the melting temperature ( $T_m$ ) at  $T_{max}$  to be  $65$  °C. No other transitions were evidenced in the thermal analysis of this material. Concerning neat castor oil-derived PU foams, besides the beta transition, an endothermic peak could also be observed at  $60$  °C, which agrees with other works reported in the literature [68, 69]. The reduced intensity of this peak may be attributed to the lower cross-linking intensity during reactive compounding, which enhanced the molecules' mobility [70]. The introduction of açai waste into the biocomposites at the lowest concentrations (5 and 10 wt%) promoted a continuous

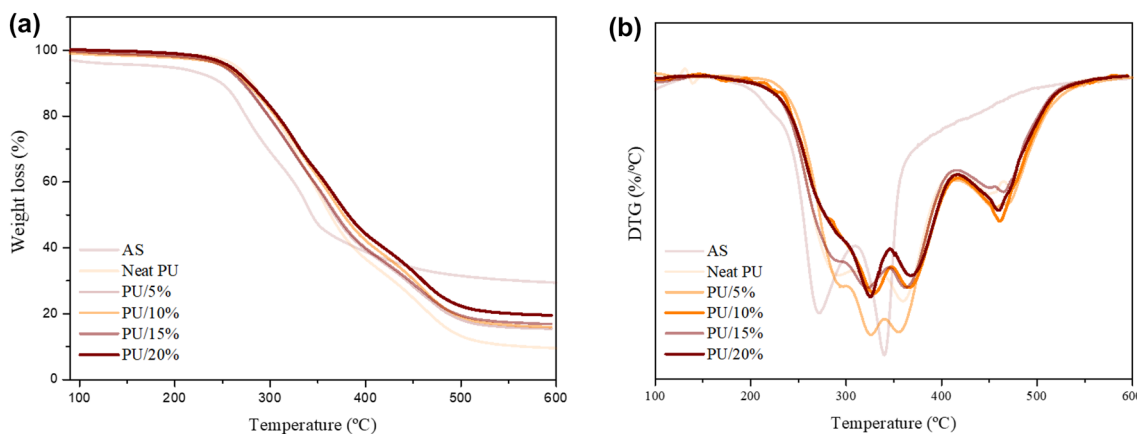


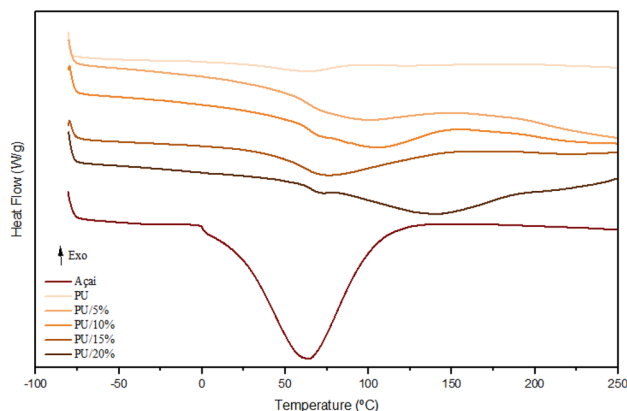
**Fig. 9** TGA (a) and DTG (b) curves of açai seed fiber, neat PU, and biocomposites samples

**Table 5** Weight loss in the range of 100–600 °C, residue (%), and  $T_{onset}$  (°C)

Samples	Weight loss (%)						Residue (%)	Tonset (°C)
	100 °C	200 °C	300 °C	400 °C	500 °C	600 °C		
Açai fiber	3.4	5.4	30.9	61.2	68.5	70.6	29.4	240
PU	0.2	1.1	17.9	63.4	86.8	90.5	9.5	266
PU/5%	0.4	1.2	20.9	60.6	81.8	84.6	15.4	257
PU/10%	1.1	2.3	17.9	57.7	81.0	81.0	16.0	263
PU/15%	0.5	1.9	20.7	60.1	80.6	83.2	16.5	260
PU/20%	0.0	1.0	17.2	55.7	77.7	80.5	19.5	272

**Table 6**  $T_5$  and  $T_{30}$  values used to obtain the heat-resistance index ( $T_{HRI}$ )

Samples	$T_5$ (°C)	$T_{30}$ (°C)	$T_{HRI}$ (°C)
PU	251	320	143.3
PU/5%	254	322	144.5
PU/10%	252	330	146.4
PU/15%	251	322	143.9
PU/20%	258	331	147.9

**Fig. 10** DSC thermograms of neat PU foam and açai waste fiber, neat PU, and biocomposites

decrease in the transition curve. However, a clear and broad endothermic peak is observed, which shifted to higher temperatures than neat PU foam. When 20 wt% of açai was added, distinct endothermic peaks were formed, evidencing the presence of the two components in the biocomposite. The high concentration of fiber seems to have limited its interaction with the PU macromolecules.

In contrast, analyzing results obtained in Fig. 11b, it was noted that samples with a higher density (PU/10%, PU/15%

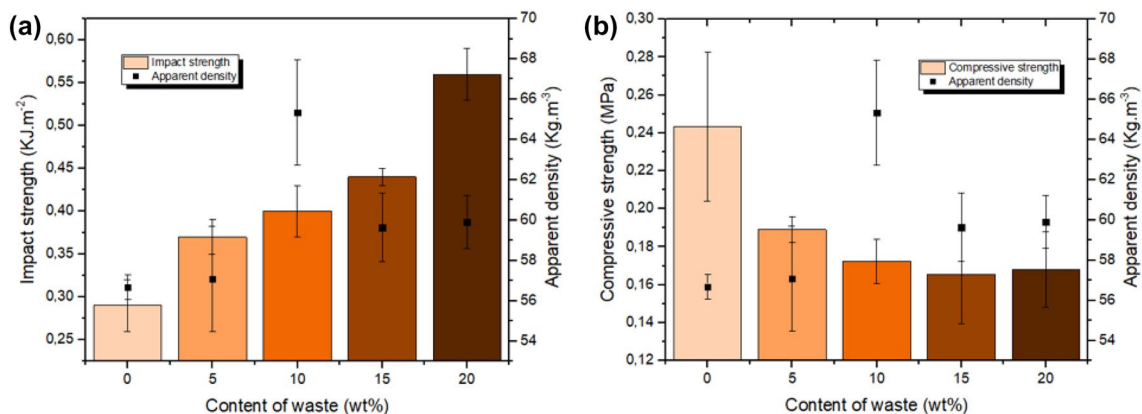
and, PU/20%) presented smaller compressive strength. The morphology of PU foams may explain this. Samples of neat PU and PU/5% possess a closed-cell structure that provides superior support to resist the compressive load. However, at higher contents of fiber, the cell structure of the foams presents a greater amount of open cells, which can reduce the cross-linking density of the matrix and hence deteriorate the mechanical properties of the materials [71]. A similar trend was reported by other studies [71–73].

## Mechanical tests

When studying the performance of PU foams, it is essential to evaluate their mechanical properties, such as impact and compressive strengths [51]. Both mechanical properties are influenced by the apparent density and morphology of the foams [71]. Figure 11 evidences the relationship between apparent density values, the content of fiber with the impact and compressive strength of the neat PU, and biocomposites. Table 7 elucidates the impact and compressive strength of materials.

Apparent density is a relevant parameter that affects the properties of PU foam and its biocomposites [44]. According to Fig. 11, it was noted that the insertion of the fiber influences the density values. The increase in density values did not occur gradually, and this can be explained by the relation between the dispersion of fiber and the viscosity of polyurethane. In high viscosity systems, the mixing process of the reagents is more challenging [22]. Consequently, the dispersion of the fibers occurs in a heterogeneous way, resulting in density variation.

Figure 11a shows that the impact strength intensified with the increasing content of açai fiber. Compared to neat PU, biocomposites presented a slight improvement in strength; thus, PU/20% biocomposite presented superior strength to other materials. In this context, the insertion of natural fibers as the reinforcement of polyurethane foams is a factor for

**Fig. 11** The behavior on the impact strength (a) and compressive strength (b) of the neat PU and biocomposites

**Table 7** Impact strength of neat PU and biocomposites

Samples	Impact strength (KJ m <sup>-2</sup> )	Compressive strength (MPa)
Neat PU	0.29 ± 0.03	0.24 ± 0.04
PU/5%	0.37 ± 0.02	0.19 ± 0.01
PU/10%	0.40 ± 0.03	0.17 ± 0.01
PU/15%	0.44 ± 0.01	0.16 ± 0.03
PU/20%	0.56 ± 0.03	0.17 ± 0.02

increased impact resistance [74], explained by the fact that the fiber behaves as a barrier in the PU matrix, enhancing the deformability as the higher content of fiber is incorporated [43, 75]. Similar findings were seen by Costa et al. [43] in jatoba shell fiber used as a filler in polyurethane foam, which showed that the impact strength increased with increasing content of natural fiber.

In contrast, analyzing results obtained in Fig. 11b, it was noted that samples with a higher density (PU/10%, PU/15% and, PU/20%) presented smaller compressive strength. The morphology of PU foams may explain this. Samples of neat PU and PU/5% possess a closed-cell structure that provides superior support to resist the compressive load. However, at higher contents of fiber, the foam's cell structure can present a greater amount of open cells, which can reduce the cross-linking density of the matrix and hence deteriorate the mechanical properties of the materials [71]. A similar trend was reported by other studies [71–73].

The stress–strain curve for PU/X% biocomposites was also evaluated, as shown in Figure S2. It can be observed that neat PU obtained a higher mechanical strength when compared to biocomposites, and this fact can be caused by inhomogeneous dispersion of açai fibers in the polymeric matrix as described in “Morphological analysis and density”. According to Mustafov et al. [76], the insertion of reinforcement in the PU matrix improves the mechanical strength of materials. However, it depends mainly on particle shape, size, and dispersion. These authors obtained similar curve profiles with the addition of diatomite and hydroxyapatite as dispersant phases in the polyurethane matrix. Literature evidences that the increase in reinforcement content results in good toughness of specimens demanding more energy to deform them [76, 77].

## Conclusion

Castor oil-based polyurethane reinforced with açai waste (5–20 wt%) biocomposites was produced and characterized as an alternative for eco-efficient building insulation. The addition of açai fiber to PU changed the pore structure, decreasing the foam cell size due to the increased

cross-link density of PU foams. Also, the fibers were hydrogen bonded to the PU molecular chains via the interaction between the O–H of the fibers and the N–H of the PU foam. Furthermore, the water absorption of the biocomposites increased with time and as a function of fiber content but did not surpass pure PU. The addition of fibers to PU also improved the crystallinity and hydrophobicity. An increase in the thermal resistance of biocomposites was observed, except for PU/15%. The compressive strength presented a decreasing trend, while, for the impact test, an increase was observed proportionally to the açai residue content. The biocomposites obtained in this work can be a candidate for building insulation.

**Supplementary Information** The online version contains supplementary material available at <https://doi.org/10.1007/s10163-021-01341-1>.

**Acknowledgements** This research was funded by Fundação Carlos Chagas de Amparo à Pesquisa do Estado do Rio de Janeiro—FAPERJ (E-26/010.101232/2018 and E-26/010.001800/2015).

## References

- Adamus J, Pomada M (2020) Selected issues of choosing composite materials for window supporting beams. *J Build Eng* 32:101542. <https://doi.org/10.1016/j.jobbe.2020.101542>
- Andersons J, Kirpluks M, Cabulis P et al (2020) Bio-based rigid high-density polyurethane foams as a structural thermal break material. *Constr Build Mater* 260:120471. <https://doi.org/10.1016/j.conbuildmat.2020.120471>
- Ikutegbe CA, Farid MM (2020) Application of phase change material foam composites in the built environment: a critical review. *Renew Sustain Energy Rev* 131:110008. <https://doi.org/10.1016/j.rser.2020.110008>
- Kuranchie C, Yaya A, Bensah YD (2021) The effect of natural fibre reinforcement on polyurethane composite foams—a review. *Sci Afr* 11:e00722. <https://doi.org/10.1016/j.sciaf.2021.e00722>
- Jamaluddin JF, Firouzi A, Islam MR, Yahaya ANA (2020) Effects of luffa and glass fibers in polyurethane-based ternary sandwich composites for building materials. *SN Appl Sci* 2:1–10. <https://doi.org/10.1007/s42452-020-3037-0>
- Pessôa TS, de Lima Ferreira LE, da Silva MP et al (2019) Açai waste benefiting by gasification process and its employment in the treatment of synthetic and raw textile wastewater. *J Clean Prod* 240:118047. <https://doi.org/10.1016/j.jclepro.2019.118047>
- Martins LS, Silva NGS, Claro AM et al (2021) Insight on açai seed biomass economy and waste cooking oil: eco-sorbent castor oil-based. *J Environ Manag* 293:112803. <https://doi.org/10.1016/j.jenvman.2021.112803>
- Ganguly P, Sengupta S, Das P, Bhowal A (2020) Valorization of food waste: extraction of cellulose, lignin and their application in energy use and water treatment. *Fuel* 280:118581. <https://doi.org/10.1016/j.fuel.2020.118581>
- Barszczewska-Rybarek I, Jaszcz K, Chladek G et al (2021) Characterization of changes in structural, physicochemical and mechanical properties of rigid polyurethane building insulation after thermal aging in air and seawater. *Polym Bull*. <https://doi.org/10.1007/s00289-021-03632-x>

10. Manobala KS, Prabhakaran S, Gautham R et al (2020) Investigation of mechanical and thermal behaviour of natural sandwich composite materials for partition walls. *Int J Res Rev* 7:211–216
11. Gurgel D, Bresolin D, Sayer C et al (2021) Flexible polyurethane foams produced from industrial residues and castor oil. *Ind Crops Prod* 164:113377. <https://doi.org/10.1016/j.indcrop.2021.113377>
12. Bresolin D, Valério A, de Oliveira D et al (2018) Polyurethane foams based on biopolyols from castor oil and glycerol. *J Polym Environ* 26:2467–2475. <https://doi.org/10.1007/s10924-017-1138-7>
13. Sharma C, Edatholath SS, Raman Unni A et al (2016) A pre-polyaddition mediation of castor oil for polyurethane formation. *J Appl Polym Sci* 133:1–9. <https://doi.org/10.1002/app.43964>
14. Hussain Shaik A, Jain R, Manchikanti S et al (2020) Reinstating structural stability of castor oil based flexible polyurethane foam using glycerol. *ChemistrySelect* 5:3959–3964. <https://doi.org/10.1002/slct.202000784>
15. Shaik AH, Banerjee S, Rahaman A et al (2021) One-step synthesis and characteristics of LiOH-castor oil based stable polyurethane foam. *J Polym Res* 28:1–9. <https://doi.org/10.1007/s10965-021-02580-4>
16. Sharma C, Kumar S, Unni AR et al (2014) Foam stability and polymer phase morphology of flexible polyurethane foams synthesized from castor oil. *J Appl Polym Sci* 131:8420–8427. <https://doi.org/10.1002/app.40668>
17. Peyrton J, Averous L (2021) Structure-properties relationships of cellular materials from biobased polyurethane foams. *Mater Sci Eng R Rep*. <https://doi.org/10.1016/j.mser.2021.100608>
18. Shao H, Zhang Q, Liu H et al (2020) Renewable natural resources reinforced polyurethane foam for use of lightweight thermal insulation. *Mater Res Express*. <https://doi.org/10.1088/2053-1591/ab8d87>
19. Calderoñ V, Gutiérrez-González S, Gadea J et al (2018) Construction applications of polyurethane foam wastes. *Recycl Polyurethane Foam*. <https://doi.org/10.1016/b978-0-323-51133-9.00010-3>
20. Gandara M, Mulinari DR, Monticeli FM, Capri MR (2020) Sugarcane bagasse fibers reinforced in polyurethane for sorption of vegetal oil. *J Nat Fibers*. <https://doi.org/10.1080/15440478.2019.1710653>
21. Mosiewicki MA, Dell'Arciprete GA, Aranguren MI, Marcovich NE (2009) Polyurethane foams obtained from castor oil-based polyol and filled with wood flour. *J Compos Mater* 43:3057–3072. <https://doi.org/10.1177/0021998309345342>
22. Martins LS, Maciel F, Mulinari DR (2020) Influence of the granulometry and fiber content of palm residues on the diesel S-10 oil sorption in polyurethane/palm fiber biocomposites. *Results Mater*. <https://doi.org/10.1016/j.rinma.2020.100143>
23. Silva NGS, Cortat LICO, Orlando D, Mulinari DR (2020) Evaluation of rubber powder waste as reinforcement of the polyurethane derived from castor oil. *Waste Manag* 116:131–139. <https://doi.org/10.1016/j.wasman.2020.07.032>
24. Li M, Pu Y, Thomas VM et al (2020) Recent advancements of plant-based natural fiber-reinforced composites and their applications. *Compos Part B Eng*. <https://doi.org/10.1016/j.compositesb.2020.108254>
25. Hung Anh LD, Pásztor Z (2021) An overview of factors influencing thermal conductivity of building insulation materials. *J Build Eng*. <https://doi.org/10.1016/j.jobte.2021.102604>
26. Zanini NC, de Souza AG, Barbosa RFS et al (2021) A novel hybrid polyurethane composites with ZnO particles and sheath palm residues: synergistic effect. *Polym Compos* 42:532–542. <https://doi.org/10.1002/pc.25845>
27. Vieira Amorim F, José Ribeiro Padilha R, Maria Vinhas G et al (2021) Development of hydrophobic polyurethane/castor oil biocomposites with agroindustrial residues for sorption of oils and organic solvents. *J Colloid Interface Sci* 581:442–454. <https://doi.org/10.1016/j.jcis.2020.07.091>
28. Husainie SM, Deng X, Ghalia MA et al (2021) Natural fillers as reinforcement for closed-molded polyurethane foam plaques: mechanical, morphological, and thermal properties. *Mater Today Commun* 27:102187. <https://doi.org/10.1016/j.mtcomm.2021.102187>
29. Moshi AAM, Ravindran D, Bharathi SRS et al (2020) Characterization of a new cellulosic natural fiber extracted from the root of *Ficus religiosa* tree. *Int J Biol Macromol* 142:212–221. <https://doi.org/10.1016/j.ijbiomac.2019.09.094>
30. Stanzione M, Oliviero M, Cocca M et al (2020) Tuning of polyurethane foam mechanical and thermal properties using ball-milled cellulose. *Carbohydr Polym* 231:115772. <https://doi.org/10.1016/j.carbpol.2019.115772>
31. Cortat LO, Zanini NC, Barbosa RFS et al (2021) A sustainable perspective for macadamia nutshell residues revalorization by green composites development. *J Polym Environ*. <https://doi.org/10.1007/s10924-021-02080-y>
32. Icduygu MG, Asilturk M, Yalcinkaya MA et al (2019) Three-dimensional nano-morphology of carbon nanotube/epoxy filled poly(methyl methacrylate) microcapsules. *Materials (Basel)* 12:1–26
33. Barbosa ADM, Rebelo VSM, Martorano LG, Giacon VM (2019) Characterization of acai waste particles for civil construction use. *Rev Mater*. <https://doi.org/10.1590/s1517-707620190003.0750>
34. Danso H, Martinson DB, Ali M, Williams J (2015) Effect of fibre aspect ratio on mechanical properties of soil building blocks. *Constr Build Mater* 83:314–319. <https://doi.org/10.1016/j.conbuildmat.2015.03.039>
35. Maia LS, Zanini NC, Claro AM et al (2021) Eco-friendly foams of castor oil based-polyurethane with Artemisia residue fillers for discarded vegetable oil sorption. *J Appl Polym Sci*. <https://doi.org/10.1002/app.51259>
36. Gonçalves Junior AC, Coelho GF, Schwantes D et al (2016) Biosorption of Cu (II) and Zn (II) with açai endocarp *Euterpe oleracea* M. in contaminated aqueous solution. *Acta Sci Technol* 38:361–370. <https://doi.org/10.4025/actascitechnol.v38i3.28294>
37. Tavares FDCF, De Almeida MDC, da Silva JAP et al (2020) Thermal treatment of açai (*Euterpe oleracea*) fiber for composite reinforcement. *Polimeros*. <https://doi.org/10.1590/0104-1428.09819>
38. Olcay H, Kocak ED (2021) Rice plant waste reinforced polyurethane composites for use as the acoustic absorption material. *Appl Acoust* 173:107733. <https://doi.org/10.1016/j.apacoust.2020.107733>
39. Członka S, Strakowska A, Pospiech P, Strzelec K (2020) Effects of chemically treated eucalyptus fibers on mechanical, thermal and insulating properties of polyurethane composite foams. *Materials (Basel)*. <https://doi.org/10.3390/MA13071781>
40. Protzek GR, Magalhães WLE, Bittencourt PRS et al (2019) The influence of fiber size on the behavior of the araucaria pine nut shell/PU composite. *Polimeros* 29:1–9. <https://doi.org/10.1590/0104-1428.01218>
41. Soberi NSM, Rozyanty AR, Zainuddin F, Osman AF (2019) Influence of filler content and mixing time on the properties and morphology of kenaf/polyurethane foam composites. *IOP Conf Ser Mater Sci Eng*. <https://doi.org/10.1088/1757-899X/701/1/012043>
42. Pearson A, Naguib HE (2017) Novel polyurethane elastomeric composites reinforced with alumina, aramid, and poly(p-phenylene-2,6-benzobisoxazole) short fibers, development and characterization of the thermal and dynamic mechanical properties. *Compos Part B Eng* 122:192–201. <https://doi.org/10.1016/j.compositesb.2017.04.017>
43. Costa ILM, Martins LS, Maia LS, Mulinari DR (2021) Impact of the Jatoba shell residue amount on polyurethane foams based on castor

- polyol. *J Mater Cycles Waste Manag* 23:1431–1444. <https://doi.org/10.1007/s10163-021-01224-5>
44. Zanini NC, de Souza AG, Barbosa RFS et al (2021) Eco-friendly composites of polyurethane and sheath palm residues. *J Cell Plast*. <https://doi.org/10.1177/0021955X20987150>
  45. Oushabi A, Sair S, Abboud Y et al (2017) An experimental investigation on morphological, mechanical and thermal properties of date palm particles reinforced polyurethane composites as new ecological insulating materials in building. *Case Stud Constr Mater* 7:128–137. <https://doi.org/10.1016/j.cscm.2017.06.002>
  46. Andersons J, Kirpluks M, Cabulis U (2020) Reinforcement efficiency of cellulose microfibers for the tensile stiffness and strength of rigid low-density polyurethane foams. *Materials (Basel)* 13:1–15. <https://doi.org/10.3390/ma13122725>
  47. Czlonka S, Strakowska A, Strzelec K et al (2020) Bio-based polyurethane composite foams with improved mechanical, thermal, and antibacterial properties. *Materials (Basel)* 13:1–20. <https://doi.org/10.3390/ma13051108>
  48. Huang S, Fu Q, Yan L, Kasal B (2021) Characterization of interfacial properties between fibre and polymer matrix in composite materials—a critical review. *J Mater Res Technol* 13:1441–1484. <https://doi.org/10.1016/j.jmrt.2021.05.076>
  49. Zhou Y, Fan M, Chen L (2016) Interface and bonding mechanisms of plant fibre composites: an overview. *Compos Part B Eng* 101:31–45. <https://doi.org/10.1016/j.compositesb.2016.06.055>
  50. Costa ILM, Monticeli FM, Mulinari DR (2020) Polyurethane foam reinforced with fibers pineapple crown biocomposites for sorption of vegetable oil. *Fibers Polym* 21:1832–1840. <https://doi.org/10.1007/s12221-020-9979-4>
  51. Sair S, Oushabi A, Kammouni A et al (2018) Mechanical and thermal conductivity properties of hemp fiber reinforced polyurethane composites. *Case Stud Constr Mater* 8:203–212. <https://doi.org/10.1016/j.cscm.2018.02.001>
  52. Sylwia C, Anna S, Kairyte Agnè KA (2020) Nutmeg filler as a natural compound for the production of polyurethane composite foams with antibacterial and anti-aging properties. *Polym Test* 86:1–13. <https://doi.org/10.1016/j.polymertesting.2020.106479>
  53. Wang J, Geng G (2015) Highly recyclable superhydrophobic sponge suitable for the selective sorption of high viscosity oil from water. *Mar Pollut Bull* 97:118–124. <https://doi.org/10.1016/j.marpolbul.2015.06.026>
  54. Calegari EP, Porto JS, Angrizani CC et al (2017) Reuse of waste paper and rice hulls as filler in polymeric matrix composites. *Rev Mater*. <https://doi.org/10.1590/s1517-707620170002.0179>
  55. Radzi AM, Sapuan SM, Jawaid M, Mansor MR (2019) Water absorption, thickness swelling and thermal properties of roselle/sugar palm fibre reinforced thermoplastic polyurethane hybrid composites. *J Mater Res Technol* 8:3988–3994. <https://doi.org/10.1016/j.jmrt.2019.07.007>
  56. Atiqah A, Jawaid M, Ishak MR, Sapuan SM (2017) Moisture absorption and thickness swelling behaviour of sugar palm fibre reinforced thermoplastic polyurethane. *Procedia Eng* 184:581–586. <https://doi.org/10.1016/j.proeng.2017.04.142>
  57. Zanini N, Carneiro E, Menezes L et al (2021) Palm fibers residues from agro-industries as reinforcement in biopolymer filaments for 3D-printed scaffolds. *Fibers Polym*. <https://doi.org/10.1007/s12221-021-0936-7>
  58. Paixão WA, Martins LS, Zanini NC, Mulinari DR (2020) Modification and characterization of cellulose fibers from palm coated by ZrO<sub>2</sub>-nHO particles for sorption of dichromate ions. *J Inorg Organomet Polym Mater*. <https://doi.org/10.1007/s10904-019-01415-6>
  59. Raja AKA, Geethan KAV, Kumar SS, Kumar PS (2021) Influence of mechanical attributes, water absorption, heat deflection features and characterization of natural fibers reinforced epoxy hybrid composites for an engineering application. *Fibers Polym*. <https://doi.org/10.1007/s12221-021-0222-8>
  60. Yang J, Ching YC, Chuah CH (2019) Applications of lignocellulosic fibers and lignin in bioplastics: a review. *Polymers (Basel)* 11:1–26
  61. Kucuk F, Sismanoglu S, Kanbur Y, Tayfun U (2020) Effect of silane-modification of diatomite on its composites with thermoplastic polyurethane. *Mater Chem Phys* 256:123683. <https://doi.org/10.1016/j.matchemphys.2020.123683>
  62. Huang G, Chen F (2019) Reaction of jute fiber with isocyanate component for the production of plant fiber-reinforced polyurethane composites. *Cellulose* 26:7297–7308. <https://doi.org/10.1007/s10570-019-02612-9>
  63. de Azevedo ARG, Marvila MT, Tayeh BA et al (2021) Technological performance of açaf natural fibre reinforced cement-based mortars. *J Build Eng* 33:101675. <https://doi.org/10.1016/j.jobe.2020.101675>
  64. Saleem J, Adil Riaz M, Gordon M (2018) Oil sorbents from plastic wastes and polymers: a review. *J Hazard Mater* 341:424–437. <https://doi.org/10.1016/j.jhazmat.2017.07.072>
  65. Asim M, Paridah MT, Chandrasekar M et al (2020) Thermal stability of natural fibers and their polymer composites. *Iran Polym J* 29:625–648. <https://doi.org/10.1007/s13726-020-00824-6>
  66. Czlonka S, Strakowska A, Pospiech P, Strzelec K (2020) Effects of chemically treated eucalyptus fibers on mechanical, thermal and insulating properties of polyurethane composite foams. *Materials (Basel)* 13:1781. <https://doi.org/10.3390/ma13071781>
  67. Gu R, Sain MM, Konar SK (2013) A feasibility study of polyurethane composite foam with added hardwood pulp. *Ind Crops Prod* 42:273–279. <https://doi.org/10.1016/j.indcrop.2012.06.006>
  68. Gu R, Khazabi M, Sain M (2011) Fiber reinforced soy-based polyurethane spray foam insulation. Part 2: Thermal and mechanical properties. *BioResources* 6:3775–3790
  69. Malik M, Kaur R (2018) Mechanical and thermal properties of castor oil-based polyurethane adhesive: effect of TiO<sub>2</sub> filler. *Adv Polym Technol* 37:24–30. <https://doi.org/10.1002/adv.21637>
  70. Njuguna JK, Muchiri P, Karuri NW et al (2021) Determination of thermo-mechanical properties of recycled polyurethane from glycolysis polyol. *Sci African* 12:e00755. <https://doi.org/10.1016/j.sciaf.2021.e00755>
  71. Czlonka S, Strakowska A, Kairyte A (2020) Effect of walnut shells and silanized walnut shells on the mechanical and thermal properties of rigid polyurethane foams. *Polym Test*. <https://doi.org/10.1016/j.polymertesting.2020.106534>
  72. Jabber LJY, Grumo JC, Alguo AC et al (2020) Influence of cellulose fibers extracted from pineapple (*Ananas comosus*) leaf to the mechanical properties of rigid polyurethane foam. *Mater Today Proc*. <https://doi.org/10.1016/j.matpr.2020.07.566>
  73. Li J, Jiang J, Xu J et al (2016) Branched polyols based on oleic acid for production of polyurethane foams reinforced with bamboo fiber. *Iran Polym J (Eng Ed)* 25:811–822. <https://doi.org/10.1007/s13726-016-0469-x>
  74. Radzi AM, Sapuan SM, Jawaid M, Mansor MR (2017) Influence of fibre contents on mechanical and thermal properties of roselle fibre reinforced polyurethane composites. *Fibers Polym* 18:1353–1358. <https://doi.org/10.1007/s12221-017-7311-8>
  75. Afzaluddin A, Jawaid M, Salit MS, Ishak MR (2019) Physical and mechanical properties of sugar palm/glass fiber reinforced thermoplastic polyurethane hybrid composites. *J Mater Res Technol* 8:950–959. <https://doi.org/10.1016/j.jmrt.2018.04.024>
  76. Mustafov SD, Sen F, Seydibeyoglu MO (2020) Preparation and characterization of diatomite and hydroxyapatite reinforced porous

- polyurethane foam biocomposites. *Sci Rep* 10:1–9. <https://doi.org/10.1038/s41598-020-70421-3>
77. Wei J, Kong F, Liu J et al (2018) Effect of sisal fiber and polyurethane admixture on the strength and mechanical behavior of sand. *Polymers (Basel)* 10:1–15. <https://doi.org/10.3390/polym10101121>

**Publisher's Note** Springer Nature remains neutral with regard to jurisdictional claims in published maps and institutional affiliations.